INTERCOMPARISON OF IMAGING SPECTROMETERS OVER THE SALAR DE UYUNI (BOLIVIA)

Marc BOUVET[(1)]

[(1)]*ESA/ESTEC, Keplerlaan 1, PB 299, NL-2200 AG Noordwijk, The Netherlands, Email: marc.bouvet@esa.int*

ABSTRACT

A-MODIS, AATSR, MERIS, POLDER-3 and SeaWiFS data are directly compared at top of the atmosphere level for nearly concomitant observation carried out under nearly identical or reciprocal geometries. Comparisons are carried out over the Salar de Uyuni in Bolivia. The results indicate that MERIS and A-MODIS are radiometrically in line. In comparison to these sensors, the SeaWiFS data exhibit a systematic underestimation of TOA reflectances of approximately 10 % in all bands. AATSR compares relatively well to MERIS and A-MODIS but shows a rapid decrease of sensitivity in 2005. The results of these intercomparisons also seem to indicate a degradation of the POLDER-3 sensitivity of several percent through its first year of operation.

1 INTRODUCTION

In order to effectively monitor Earth climate change indicators, it is essential that the multitude of observations made by different sensors onboard space platforms, are made comparable. With emerging large-scale initiatives involving more space agencies and member states such as the Global Earth Observation System of Systems (GEOSS), the need for interoperability, data merging and data continuity is growing. Ensuring that the calibration differences between sensors are understood and well quantified is an essential step in the implementation of a long-term global monitoring plan. The joint European Space Agency (ESA) / European Union initiative on Global Monitoring for Environment and Securing (GMES) can only be successful if the operational services provided by satellites attain the requisite quality through adequately calibrated and validated data to analyze long-term trends in the Earth's environment and climate.

Various imaging spectrometers are currently acquiring global data of the Earth in the visible to NIR electromagnetic spectrum with a three-fold mission objective: ocean, land and atmosphere monitoring. Among them, the Medium Resolution Imaging Spectrometer (MERIS) and the Advanced Along Track Scanning Radiometer (AATSR) both on the ESA platform ENVISAT, the Polarization and Directionality of the Earth's Reflectances (POLDER-3) on the CNES PARASOL platform, the Moderate Resolution Imaging Spectro-radiometer on the NASA satellite Aqua (A-MODIS) and the Sea Viewing Wide Field Spectrometer (SeaWiFS) on the NASA Orbview-2. Because all five missions share similarities, their data are naturally inclined to be compared or merged.

The prerequisite to the comparison of these data and their synergetic merging is to understand the differences at calibration level between these sensors.

While AATSR, A-MODIS, MERIS and SeaWiFS possess onboard calibration devices characterized prior to launch (R 1, R 2, R 21, R 25, R 26), the POLDER-3 instrument relies on vicarious calibration only (R 11).

Because the radiometric accuracy requirements for ocean colour are highly demanding, *absolute vicarious calibration* for these missions is a challenging task. Using the reflectance-based method over bright surfaces, various investigators claim accuracies at top-of-atmosphere (TOA) reflectance level of few percents in the visible to red spectral range (R 18, R 16). Over targets where the surface reflective properties can be guessed a priori, such as oligotrophic dark ocean targets, similar accuracies are claimed (R 12).

The lack of in-situ measurements describing the atmosphere/surface physical state is a strong limitation when trying to achieve *absolute calibration* over natural targets. Workarounds exists to cope with the lack of in-situ data availability and still be able to retrieve pertinent information. There are, in fact, vicarious calibration methodologies that can be referred to as *intercalibration* methodologies for which several sensors data are intercompared over a bright natural target and one of the sensors is arbitrarily chosen as a reference (R 6, R 4). This type of methodology, if operationally implemented, can provide long time series of relative differences in instrument calibration that can be nailed down to an absolute reflectance scale by episodic absolute calibration experiments. Hereafter is presented an attempt to identify trends over nearly 4 years of operations in the relative differences of radiometric calibration between A-MODIS, AATSR MERIS, POLDER-3 and SeaWiFS. The natural target chosen for this intercomparison is the *Salar de Uyuni* (Bolivia). It was selected for its spectrally white high reflectance, its flatness, its high altitude location and its dry climate. In the next section, the details of the methodology are described. Then, the results are presented and discussed.

Proceedings of the Second Working Meeting on MERIS and AATSR Calibration and Geophysical Validation (MAVT-2006), 20-24 March 2006, ESRIN, Frascati, Italy (ESA SP-615, July 2006)

2 METHODOLOGY

2.1 The methodology

The goal of the methodology could be simplistically summarized as follow: *to identify radiometric calibration differences between two different sensors by looking at the same terrestrial target from the top of the atmosphere, at the same time and in the same geometrical configuration*. L1B radiance/reflectance data in all available bands spanning from the 400 nm to 1020 nm are systematically extracted from A-MODIS, AATSR, MERIS, POLDER-3 and SeaWiFS data over a region of interest of dimensions 20 km by 60 km centered on the *Salar de Uyuni*, in Bolivia. The data are then visually cloud screened and converted to a common radiometric scale (when needed): the remote sensing reflectance. This conversion is carried with the help of the extraterrestrial spectral irradiance spectrum specific to each mission and the Relative Spectral Responses (RSR) of each band from each instrument. For each acquisition from each sensor, the reflectances in all spectral bands, the sun zenith angle (SZA), the viewing zenith angle (VZA) and the viewing azimuth angle relative to the principal plane (RAA) are average over all pixels included in the region of interest and systematically stored.
Then, doublets between two sensor acquisitions *i* and *j* are searched which have comparable geometries of observation and illumination. To look for such doublets, it is assumed that the TOA reflectance angular distribution obeys a) the principle of reciprocity and b) is symmetrical with respect to the principal plane. The principal of reciprocity states that the following relationship is true:

$$\rho_i^{TOA}(SZA_i, VZA_i, RAA_i) = \rho_j^{TOA}(VZA_j, SZA_j, RAA_j) \quad (1)$$

while the symmetrical assumption with respect to the principal plane can be formulated as:

$$\rho_i^{TOA}(SZA_i, VZA_i, RAA_i) = \rho_j^{TOA}(SZA_j, SZA_j, -RAA_j) \quad (2)$$

Because an exact geometrical match is often not possible, the search for such geometrical configuration is actually carried out by looking for acquisitions between the sensor *i* and the sensors *j* satisfying the condition $\chi_{ij}<10$ where χ is defined as:

$$\chi_{ij} = \sqrt{\left([SZA_i - SZA_j] + [VZA_i - VZA_j] + \tfrac{1}{4}[|RAA_i| - |RAA_j|]\right)} \quad (3)$$

$\chi_{ij}<10$ roughly corresponds to configurations for which the SZA's, the VZA's do not differ by more than 5° and the RAA's by more than 10°.
Moreover, only doublets of two sensors that satisfy the geometrical criteria of equation (3) and for which the acquisition were performed on the same day or one day apart are kept in the final dataset. This implicitly equivalent to assuming that the TOA reflectance Bidirectional Reflectance Distribution Function (BRDF) does not vary significantly over 24 hours.
Finally, if for a given acquisitions of sensor *i,* there exists several acquisitions from sensor *j* satisfying the previous geometrical and temporal criteria, then only the matching acquisition from sensor *j* for which the χ_{ij} is the smallest is kept to form a doublet with the acquisition of sensor *i*.

2.2 Site characteristics and climatology

The Salar de Uyuni (Bolivia) is a salt lake located at approximately 20 degree South latitude and 68 degree West longitude (*Figure 1*). Only a marginal part of its surface remains wet during the dry season (March to November) thus leaving large areas of dry and highly reflective salt. In its largest dimension, it extends by approximately 200 km. It is a plateau lying at an altitude of 3600 m.
The rain season starts in December and ends up in March. The lake surface is then flooded for few months. From data obtained at a meteorological station located East of the dry lake, operated during over 13 years between 1987 and 1999 (R 15), the average precipitation is nearly null from May to October. For the same period of the year (dry season), the averaged number of rain days per month over 13 years is between 0 and 2. Mean temperatures oscillate between 14 degrees in December and 2 degrees in June.

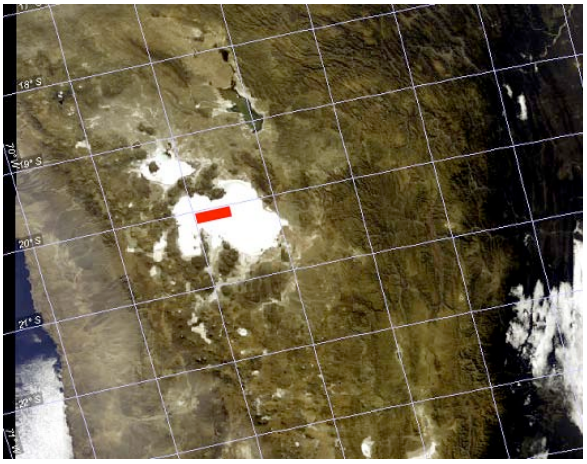

Figure 1: The Salar de Uyuni (Bolivia) as observed by MERIS on the 10th of June 2005. The region of interest chosen for intercomparison of TOA reflectances lies between latitudes -20.16 and -20.00 degree latitude and -68.05 degree and -67.45 degree longitude.

Salar de Uyuni is a large, flat and radiometrically homogenous area.

Authors of R 15 carried out ground reflectance measurements with a LICOR LI-1800 spectrometer and obtained average reflectance spectrum smoothly increasing from 70 % to 80 % between 400 nm and 900 nm. This spectrum was extracted in the area considered in the present intercomparison study. If looking at the surface at different wavelength can expect spectral reflectance gradients of about 0.025 % / nm.

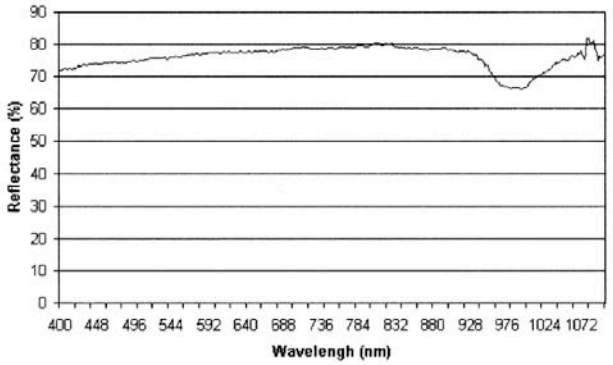

*Figure 2: Mean ground reflectance spectrum measured with the spectroradiometer LICOR LI-1800 on June 8 and June 9, 1999 (*R 15*)*

This spectral flatness minimizes differences when comparing reflectances from sensors having relative spectral responses (RSR) differing in their width or wavelength center.
The high altitude of the *salar* implies a rarefied molecular atmosphere. Pressure is approximately reduced to two thirds of the mean sea level pressure, consequently reducing the Rayleigh scattering optical thickness and thus the atmospheric influence on the downwelling and upwelling radiation field.
An interesting characteristic of a salt lake such as the *Salar de Uyuni* is that it should have a smooth BRDF and as a consequence, the differences in measured TOA reflectances when observing its surface under closely related geometries should be minimized.

2.3 The satellite data

The satellite data consist of L1B data, i.e., radiometric and geolocation/navigation data. The TOA reflectances are extracted systematically from overpasses and are further visually cloud screened. All data starting from 2002 and finishing in 2005 are included when available thus resulting in maximum 4-year time series.
For each sensor, the final radiometric quantities extracted are TOA reflectances in all spectral bands spanning from 400 nm to 1000 nm. When not available directly as reflectances, the TOA radiometric quantities (radiances or normalized reflectances) are converted into reflectance via the appropriate extraterrestrial solar irradiance E_0 and knowledge of the sun zenith angle. The final radiometric quantity thus compared is the remote sensing reflectance:

$$\rho^{TOA} = \frac{\pi L^{TOA}}{E_0 \cos(SZA)} \quad (4)$$

The Sun Zenith Angle (SZA), Sun Azimuth Angle (SAA), Viewing Zenith Angle (VZA), Viewing Azimuth Angle (VAA) were also extracted from the auxiliary navigation data in the L1B files and similarly to the TOA reflectances, they were averaged over the region of interest (*Figure 1*).

2.3.1 AATSR data

The AATSR instrument is a dual-view instrument with channels from the visible to the thermal infrared (R 17). It has a spatial resolution of approximately 1 km.
The calibration system for the reflection channels (560 nm, 670 nm and 860 nm) (VISCAL) provides a stable source for calibration once per orbit, using sunlight to illuminate a diffusing plate.
Starting from 30th of November 2005, a drift correction has been implemented in the ground processor based on vicarious calibration (R 22). All previous L1B data here presented have been processed to account for these drift corrections. The latitude and longitude corrections accounting for the target altitude were applied. The AATSR L1B reflectances were further converted into a remote sensing reflectances via the cosine of the SZA.
The data here presented cover the period from April 2002 to December 2005.

2.3.2 MERIS data

The MERIS data (R 21) here presented are L1B Reduced Resolution. MERIS radiometric and spectral calibration is based on onboard solar diffusers and the instrument spectral model was further characterized in flight (R 7*)*. The data originate from two difference processors: the MEGS PC 7.4 processor and the MERIS ground segment processor version 4.07. The difference between these two processors should not induce sensible difference at L1B radiometry level for the purpose of our study (confirmed by R 24).
In the study, the L1B data are further corrected for the *smile* effect (R 7), which refers to a spectral shift of the wavelength center for a given spectral band (and for a given pixel). In the present study, the *smile* correction was restricted to the irradiance correction (R 20*)* as justified by the small spectral variations of the surface reflectivity.
The irradiance correction was carried out and the radiances converted into reflectance via the mean annual extraterrestrial solar irradiance from R 23, the instrument RSR and the correction for the Earth Sun distance following the formulation of *Gregg and Carder*

(R 10). The latitude and longitude corrections accounting for the target altitude were applied.
The data here presented cover the period from April 2002 to December 2005 included.

2.3.3 MODIS Aqua data

MODIS Aqua data (R 14) here presented are L1B 1-km products from reprocessing 1.1. Only those spectral bands which do not saturate over bright targets in the visible spectrum are extracted, the latest bands are dedicated to the study of land processes, thus enabling *Salar de Uyuni* reflectance to be monitored. Calibration of the L1b reflective solar bands is based on an onboard solar diffuser (R 25,R 26*)*. It is important to note that the results of the intercomparison here presented cannot be interpreted in terms of differences at ocean colour products level for the former products are based on TOA radiances/atmospheric correction vicariously calibrated at the MOBY site.
The A-MODIS L1B reflectances are further converted into a remote sensing reflectance via the cosine of the SZA. The data here presented cover the period from April 2002 to December 2005 included

2.3.4 POLDER-3

The POLDER-3 level 1 product includes geolocated and TOA spectral reflectances and Stokes parameters characterizing the linear polarisation of the light (R 19). The PARASOL/POLDER radiometric model is applied to the polarized channels in order to compute the three accessible Stokes parameters. The polarization parameters observed by the polarized channels are interpolated for the other channels in order to correct the optical polarization effects and the radiances are derived for the non-polarized channels. The radiances are normalized by the incident solar flux. The POLDER-3 data have a spatial resolution of about 6 km and are provided in up to 17 directions over a given target. It is recommended to make cautious use of the 443 nm band data because of unsolved straylight issues.
The here presented L1B data were processed with radiometric (PER V2.00) and geometric (PEG V2.01) calibrations. No use of the information related to the linear polarization was made in the present study; only the total intensity of the spectral reflectances was extracted.

2.3.5 SeaWiFS

A general description of the SeaWiFS instrument can be found in R 13. SeaWiFS calibration follows a multiple approach: direct calibration and vicarious calibration (R 1, R 2*)*. TOA radiances over water surface are vicariously calibrated with the MOBY water leaving measurements propagated to the TOA (R 8*)*. Over land and clouds, the direct calibration results (preflight characterization and in-flight lunar and solar measurements) are used to calibrate the TOA radiances. The SeaWiFS data presented in this intercomparison over *Salar de Uyuni* correspond to the result of direct calibration. The results of the intercomparison here presented are not interpretable in terms of ocean color products differences. The L1A data presented in this study originate from reprocessing 5.1. The L1A data were extracted from the data archive and processed to L1B using the version 4.7 (2002 to 2004 LAC data) and 4.8 (2005 GAC data) of the SeaWiFS Data Analysis System software (SeaDAS). Since reprocessing 5.1, the extraterrestrial solar irradiance spectrum from R 23 is used to generate L1B radiances. The corresponding band averaged irradiances were applied to convert the SeaWiFS L1b radiances into TOA reflectances. Correction for the Earth Sun distance was carried out similarly to the MERIS data, following the *Gregg and Carder (*R 10*)* approach.

3 RESULTS

After cloud screening of the satellite data and conversion to the remote sensing reflectance, the grand total of acquisitions over the period 2002-2005 is 426 for A-MODIS, 324 for AATSR, 230 for MERIS, 1197 for POLDER-3 (each viewing geometry being considered as an acquisition) and 654 for SeaWiFS.
Applying the previously described geometrical and temporal criteria to identify doublets of remote sensing reflectances we obtain two types of doublets: those satisfying equation (1) which will be referred to as *identical doublets* for which geometry obeys the principal of reciprocity of equation (2) which will be referred to as *reciprocal doublets*.
The search for doublets results successful, as reported in *Table 1* where the total number of doublets (reciprocal and identical doublets) for two sensors is followed, between brackets, by the number of reciprocal doublets.

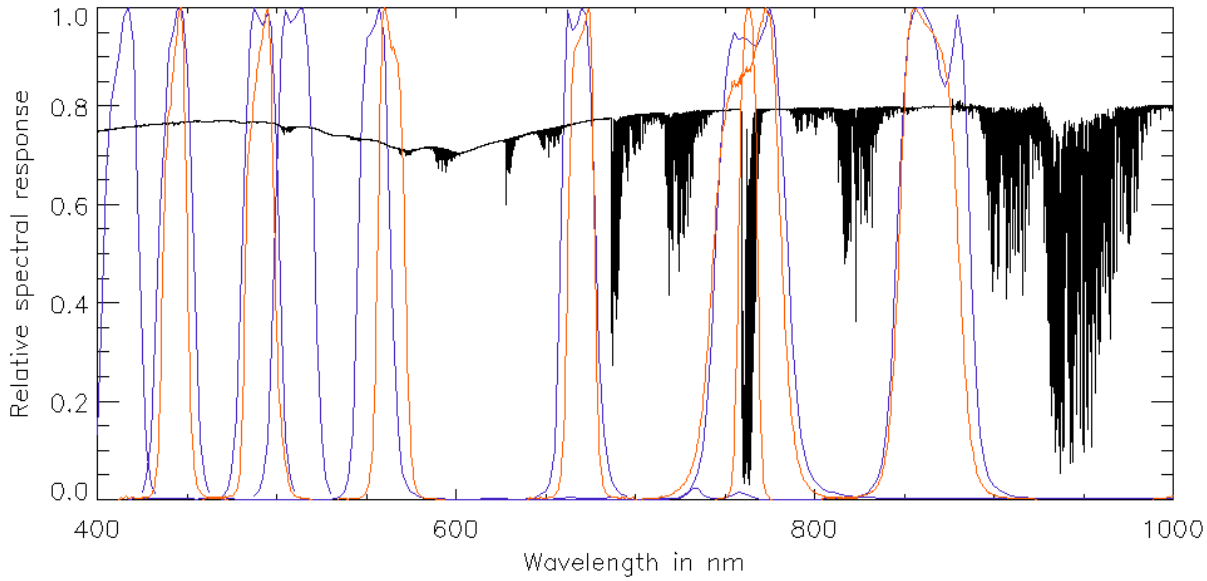

Figure 3: the Relative Spectral Response of MERIS (in blue) and POLDER-3 (in orange). Superimposed, a TOA reflectance spectrum simulated with MODTRAN for a nadir looking sensor observing a surface with a spectrally constant reflectance of 0.8, located at 3600 meters of altitude, beneath a US 1976 standard atmosphere, in aerosol free conditions, with a sun zenith angle of 50 degrees

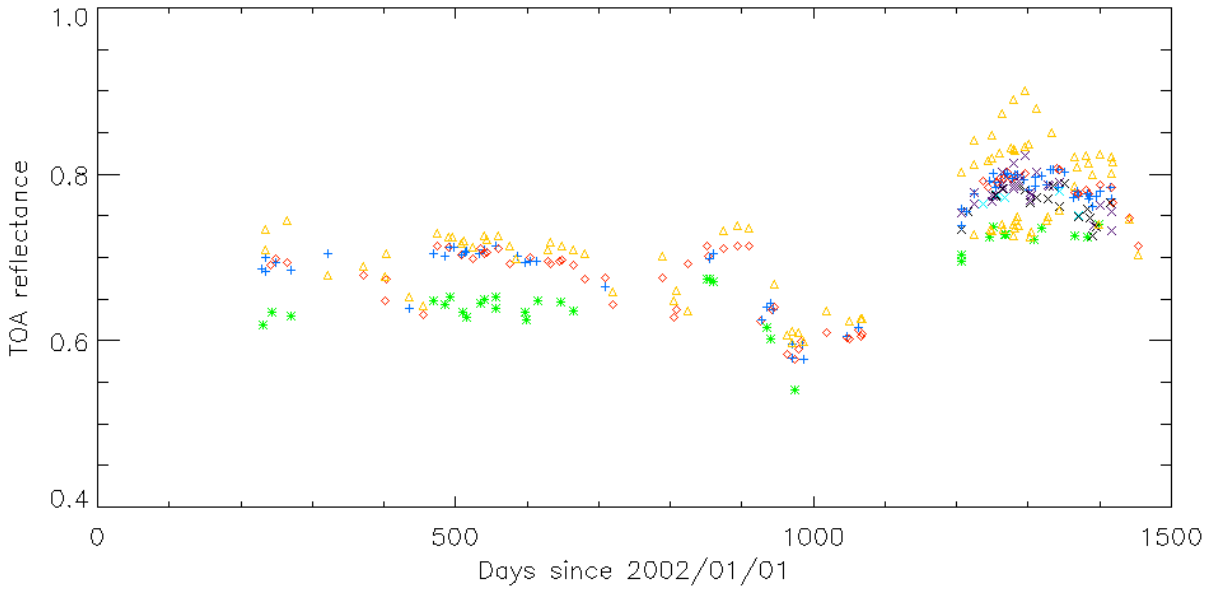

Figure 4:The time series of TOA reflectances at 865 nm from the A-MODIS (blue cross), AATSR (orange triangles), MERIS (red diamonds), POLDER-3 (purple crosses) and SeaWiFS (green stars) over the Salar de Uyuni.

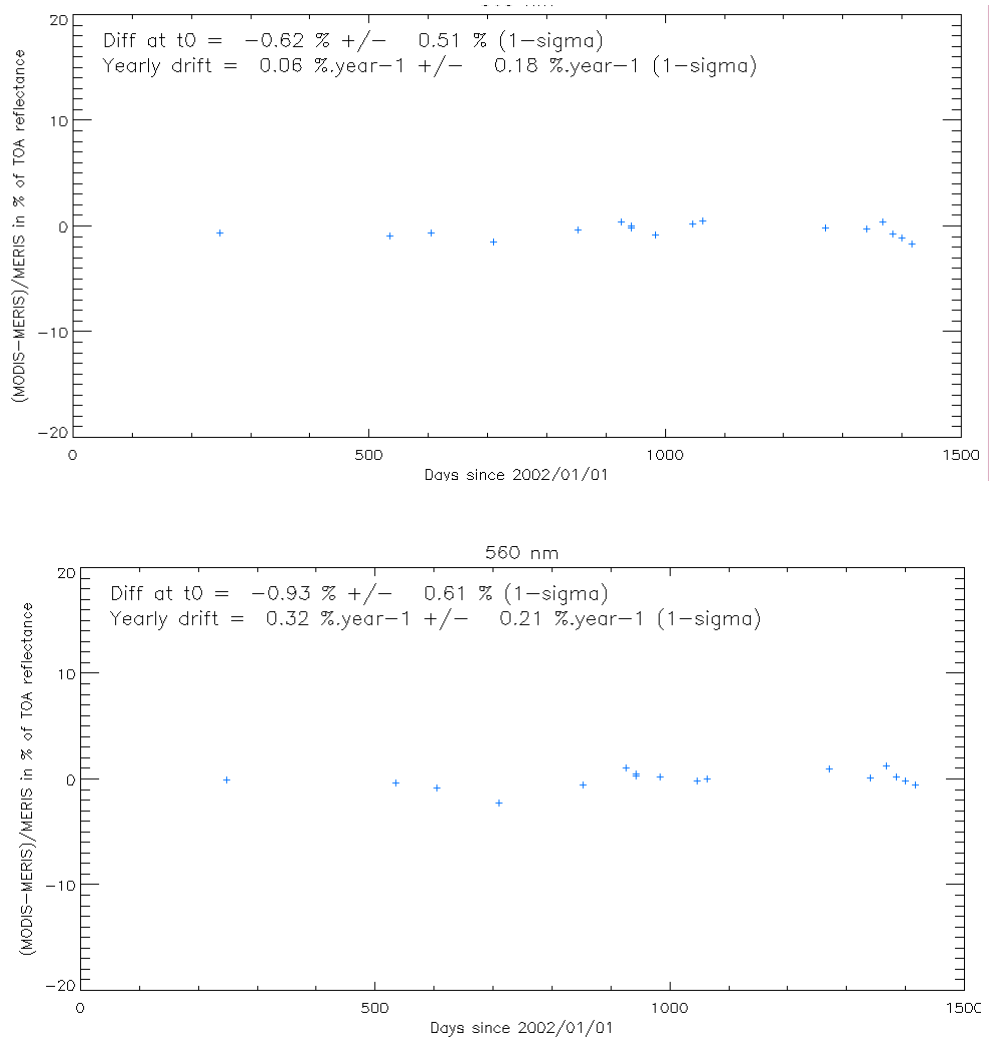

Figure 5: the relative difference of TOA reflectance between A-MODIS and MERIS: (A-MODIS-MERIS)/MERIS (in %) at 865 nm (top) and 560 nm (bottom). Also indicated the difference at t0 and the yearly drift which are respectively the ordinate at t=0 (2002/01/01) and the slope of the linear fit of the data.

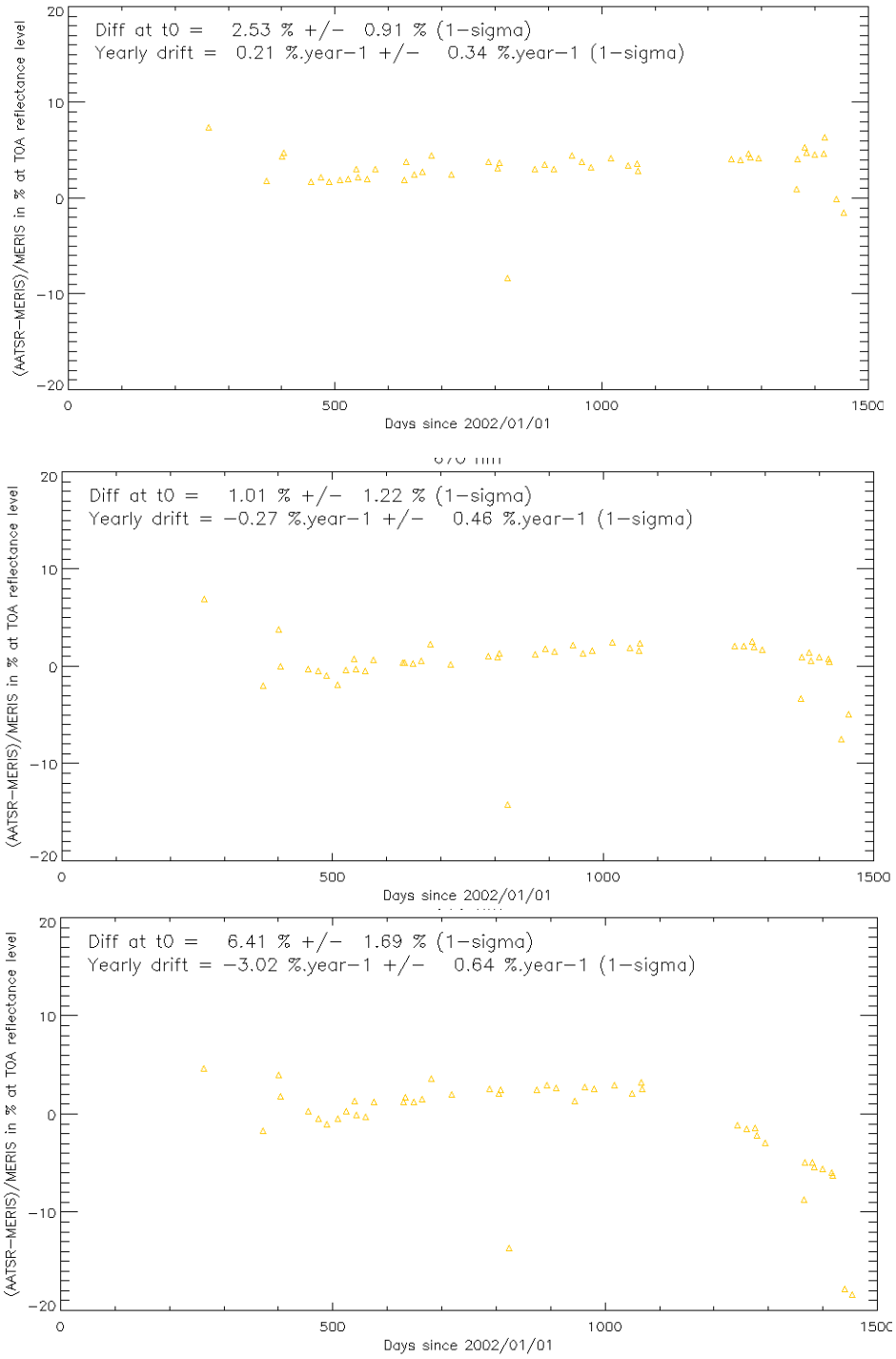

Figure 6: the relative difference of TOA reflectance between AATSR and MERIS: (AATSR-MERIS)/MERIS (in %) at 865 nm (top) 670 nm (middle) and 560 nm (bottom). Also indicated the difference at t0 and the yearly drift which are respectively the ordinate at t=0 (2002/01/01) and the slope of the linear fit of the data.

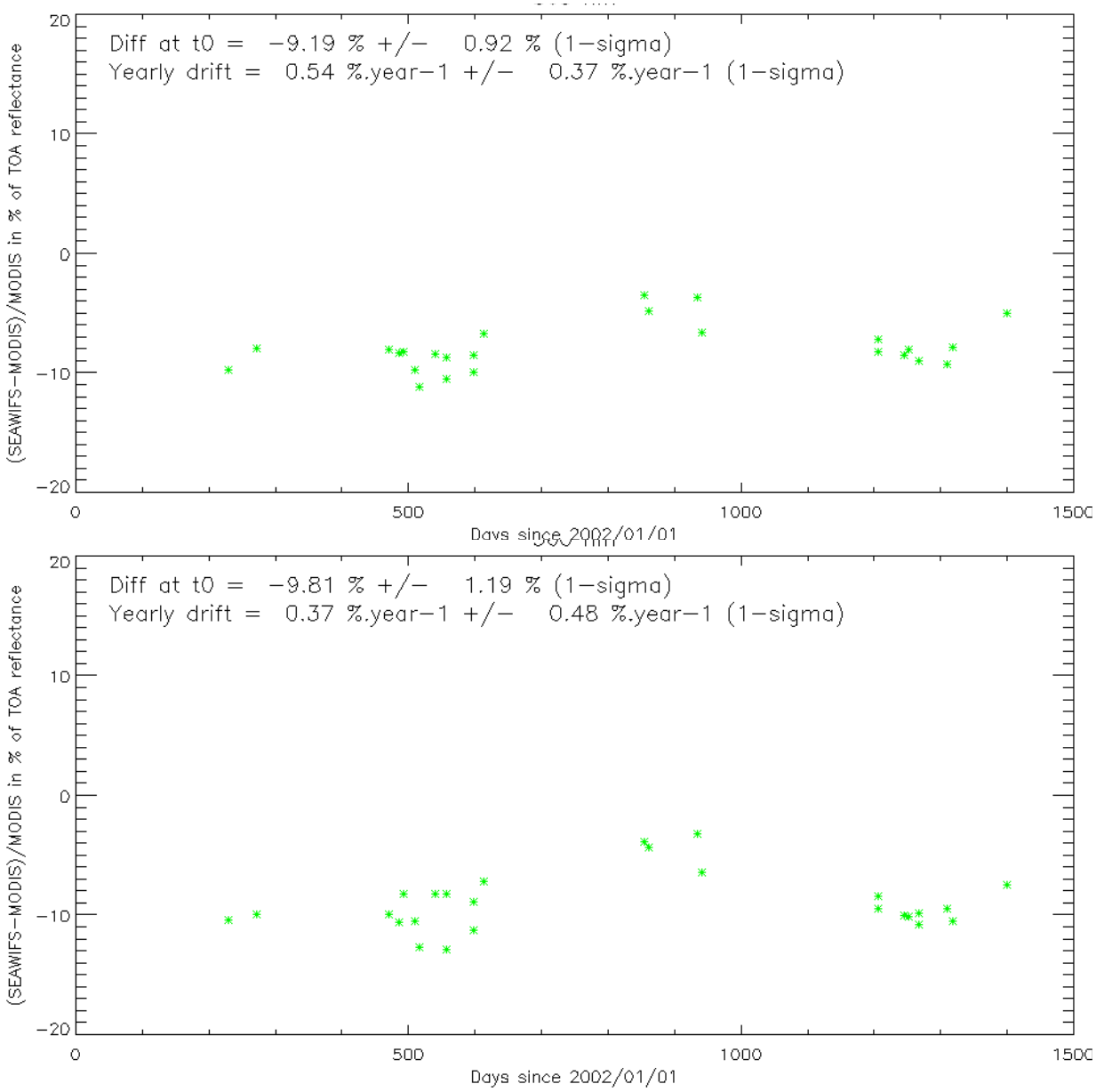

Figure 7: the relative difference of TOA reflectance between A-MODIS and SeaWiFS: (SeaWiFS-A-MODIS)/ A-MODIS (in %) at 865 nm (top) and 560 nm (bottom). Also indicated the difference at t0 and the yearly drift which are respectively the ordinate at t=0 (2002/01/01) and the slope of the linear fit of the data.

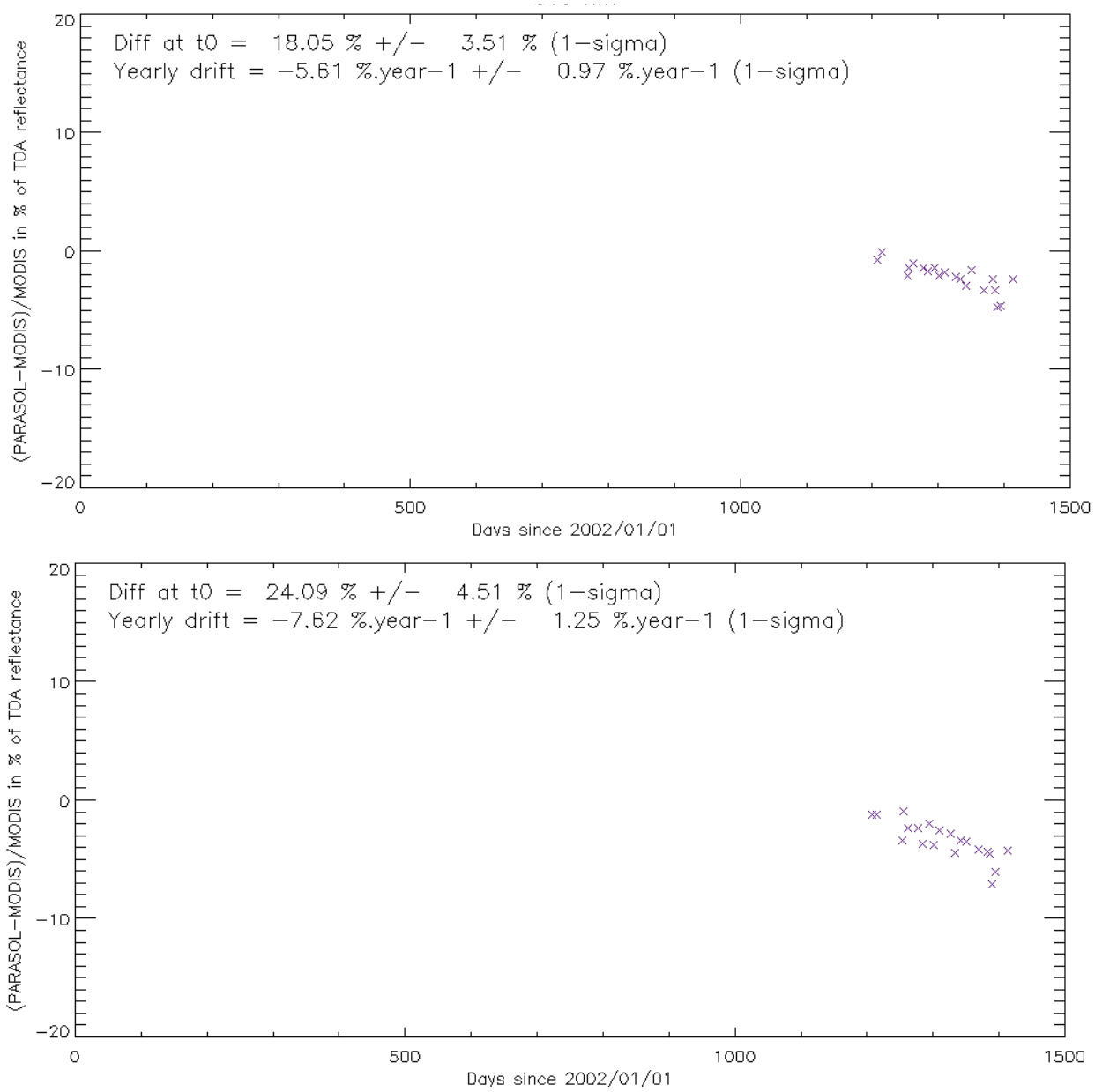

Figure 8: the relative difference of TOA reflectance between A-MODIS and POLDER-3: (POLDER-MODIS)/ MODIS (in %) at 865 nm (top) and 560 nm (bottom). Also indicated the difference at t0 and the yearly drift which are respectively the ordinate at t=0 (2002/01/01) and the slope of the linear fit of the data.

	MODIS	AATSR	MERIS	POLDER	SeaWiFS
MODIS		17 (0)	17 (4)	20 (7)	26 (26)
AATSR	17 (0)		47 (0)	11 (3)	5 (3)
MERIS	17 (4)	47 (0)		7 (0)	6 (5)
POLDER	20 (7)	11 (3)	7 (0)		17 (8)
SeaWiFS	26 (26)	5 (3)	6 (5)	17 (8)	

Table 1: The number of doublets identified between the sensors. Between brackets, the number of doublets for which the geometries of observation are reciprocal.

For each doublets, a number of spectral bands per sensor are available which can be compared to the other sensor. As can be seen on the *Table 2*, all sensors possess a spectral band centered approximately on 560 nm and 865 nm. MERIS and SeaWiFS possess 7 spectral bands sharing similarities. The A-MODIS ocean spectral bands corresponding to the MERIS/SeaWiFS spectral bands could not be used here because their radiometric gain is such that they saturate over bright targets such as the *Salar de Uyuni*.

Band	MODIS	AATSR	MERIS	POLDER	SeaWiFS
412 nm			x		x
442 nm			x	x	x
490 nm			x	x	x
510 nm			x		x
560 nm	x	x	x	x	x
670 nm		x	x	x	x
860 nm	x	x	x	x	x

Table 2: The crosses indicate the spectral bands available in this study for each sensor

Figure 4 shows the time series of all the doublets data from all sensors in the 865 nm spectral band. This figure gives an indication of the temporal variability of the surface reflectance and the associated TOA reflectance.
Figure 5 to *Figure 8* show the results of the intercomparison MERIS-A vs. MODIS, MERIS vs. AATSR, A-MODIS vs. SeaWiFS and A-MODIS vs. POLDER-3.
More intercomparison could be shown, for instance, MERIS vs. SeaWiFS but we will limit ourselves to the present cases. It is to be said that coherency between the intercomparisons can be observed in the data, for instance, the differences between A-MODIS and SeaWiFS of about 10 % at 865 nm (see *Figure 7*) are also observed between MERIS and SeaWiFS, as expected from the good agreement between MERIS and A-MODIS at this wavelength (see *Figure 5*).

4 DISCUSSION

4.1 On the validity of the principle of reciprocity

It might be objected to the general principle of the methodology described in the section 2 that the principle of reciprocity (R 5) does not necessarily apply to TOA reflectances.
There are 20 identified doublets for A-MODIS and POLDER-3. 7 of these are reciprocal doublets and 13 are identical doublets. As show in *Figure 9*, the reciprocal and identical doublets provide similar estimate of the relative difference between the TOA reflectances of A-MODIS and PODER-3. Similar results are observed when looking at intercomparisons between MERIS and A-MODIS. The principle of reciprocity appears thus to be valid within the accuracy of the methodology.

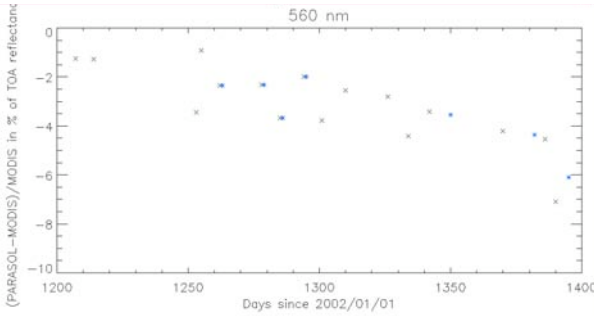

Figure 9:The relative difference at the TOA between A-MODIS and PARASOL. The reciprocal doublets (blue stars) and the identical doublets suggest a similar temporal trend.

4.2 Differences in TOA reflectances induced by the differences in RSR

The RSR of each instrument overlap for most bands but noticeable differences can be observed (see *Figure 3*). To simulate the differences at TOA reflectance level induced by the sensor-to-sensor differences in RSR, a synthetic spectrum of the *Salar de Uyuni* is generated. This spectrum is obtained from the MODTRAN radiative transfer code (R 3). It simulates the measured reflectance spectrum of a sensor looking at a spectrally white surface with a constant reflectance of 0.8, located at 3600 meters of altitude, beneath a US 1976 standard atmosphere, in aerosol free conditions, with a sun zenith angle of 50 degrees and a nadir viewing angle. From the synthetic reflectance spectrum the band average reflectance values are computed in order to assess the impact of atmospheric spectral features (gaseous absorptions) on the TOA reflectances in each band and for each sensors. *Table 3* shows that for all bands, we can expect sensors-to-sensor differences due to RSR differences below 1% in TOA

reflectance (expect for 670 nm where it reaches 1.6 %). Such conclusion is valid over the *Salar de Uyuni* only and cannot be extended to other surface.

Band	MODIS	AATSR	MERIS	POLDER	SeaWiFS
412 nm			0.7550		0.7556
442 nm			0.7655	0.7658	0.7659
490 nm			0.7673	0.7662	0.7659
510 nm			0.7567		0.7574
560 nm	0.7287	0.7253	0.7241	0.7184	0.7281
670 nm		0.7549	0.7622	0.7664	0.7643
860 nm	0.7951	0.7972	0.7976	0.7980	0.7948

Table 3: band average reflectance simulated with the instruments Relative Spectral Responses and a MODTRAN simulation for a nadir looking sensor observing a surface with a spectrally constant reflectance of 0.8, located at 3600 meters of altitude, beneath a US 1976 standard atmosphere, in aerosol free conditions, with a sun zenith angle of 50 degrees

The synthetic spectrum was generated assuming that the salt of *Salar de Uyuni* is Lambertian and has a constant reflectance over the whole spectrum. The latest hypothesis is most likely not exact. Surface reflectance spectral variations are anticipated to be of the order of 0.025% / nm as shown by R 15*(Figure 2*). The wavelength centers of the sensor bands do not differ by more than 10 nm. The spectral slope of the reflectance is thus expected to be of the order of 0.25 % at the TOA (according to *Figure 2*). It could however be larger when the lake is flooded since the presence of water induces a stead decrease of reflectance in the red and NIR. We can expect for a non-flooded surface that the differences in RSR for comparable bands will not exceed 2 %.

4.3 Sensitivity of the methodology to the accuracy of the geolocation

Geolocation errors for all sensors under study are expected to be below the 2 km scale. They are in fact claimed to within few hundred meters for MERIS and MODIS full resolution data (see, for instance, *Goryl et al. [2004]* for MERIS). For each MERIS, A-MODIS, AATSR, POLDER-3 and SeaWiFS scene, the TOA reflectances are extracted from a fixed region of interest. The region of is about 20 km by 60 km. To assess the impact of geolocalisation errors on the TOA reflectances, the region of interest was shifted by about 0.02 degree North (about 2km) and 0.02 degree West (about 2km) on a MERIS scene. The differences between the TOA spectral reflectances of the shifted region of interested and those from the non-shifted region of interested remain below 0.5 % in all spectral bands. The error due to geolocation is likely to be below this 2-km value however. It is to be noted that in the specific case of SeaWiFS, at large viewing zenith angles, the geolocation of the data seems to degrade. Based on visual inspection of the variations of position of the region of interest with respect to the lake, errors of geolocation of several kilometers were observed. This effect is clearly visible in intercomparisons involving SeaWiFS: they appear particularly noisy (*Figure 7*).

4.4 Systematic differences and random noise in time series of relative difference between two sensors TOA reflectances

As previously discussed, we can anticipate two sources of systematic relative differences when computing the difference between the TOA reflectances from two sensors (such as done in *Figure 5*, *Figure 6*, *Figure 7*, *Figure 8*): 1) those linked to the differences in spectral response (less than 2 %) and 2) those related to the accuracy of the geolocation (less than 0.5 %). These two errors combined might thus induce systematic differences of 2.5 % in the worst case (at 670 nm) in figures such as *Figure 5*, *Figure 6*, *Figure 7*, *Figure 8*. Such estimate is larger for comparisons involving SeaWiFS since its geolocation accuracy appears much lower than other sensors (over land).
The geolocation accuracy and the differences in SZA, VZA and RAA induced by the condition $\chi_{ij}<10$ (see equation (3)) are sources of random noise when looking time series of TOA reflectance differences between two sensors.
In periods when the surface of the *salar* is flooded, the methodology remains valid but systematic differences at TOA reflectance level between two sensors induced by the differences in RSR might be larger. In fact, the spectral variations of the surface reflectance should be steeper. Moreover, the large variations of the surface BRDF in geometries close to the specular reflection might induce outliers in the time series of relative differences of TOA reflectances.

4.5 Comparison of TOA reflectances from A-MODIS, AATSR, MERIS, POLDER-3 and SeaWiFS

In the light of the previous discussion, the methodology here presented provides the means to identify radiometric calibration differences larger than 2.5 % (in all comparisons not involving SeaWiFS). In specific cases, like for instance, when looking at difference between MERIS and A-MODIS TOA reflectances in the 865 nm band, the differences in relative spectral responses and the geolocation should enable identification of calibration differences below 1%.

The comparison between MERIS and A-MODIS TOA reflectances shows excellent agreement (see *Figure 5*) both at 560 nm and 865 nm. Because they compare well, they can be used indifferently in comparisons to other sensors in these two bands.

Figure 6 shows the relative differences at TOA level between MERIS and AATSR. Since they operate on the same platform, numerous simultaneous acquisitions under the same geometry are identified. Outliers are due to regular periods of outgasing of the AATSR instrument resulting into rapid changes in sensitivity of the instrument that are modeled via the on ground calibration processing. In 2005, the AATSR instrument seems to suffer a loss of sensitivity at 560 nm and 670 nm. The AATSR degradation model as not yet been updated in 2005 and might be the cause for such loss of sensitivity (personal communication D. Smith)
Figure 7 shows the relative differences at TOA between A-MODIS and SeaWiFS. The SeaWiFS TOA reflectances appear to be about 10 % below the A-MODIS TOA reflectances. Similar differences are found between MERIS and SeaWiFS TOA reflectances at 412 nm, 443 nm, 490 nm, 560 nm, 670 nm and 860 nm thus indicating a spectrally white difference of the calibration of SeaWiFS of approximately 10 % with respect to A-MODIS and MERIS. Note the large random noise associated to the time series. It is due to the degradation of the accuracy of the geolocation for large viewing angles (confirmed through visual inspection of the position of the region of interest with respect to the lake morphology).
Figure 8 shows the relative differences at TOA level between A-MODIS and POLDER-3. The time series indicates what could be a degradation of the POLDER-3 instrument in its first year of operation of 5% per year and 7 % per year respectively in the two spectral bands centered at approximately 560 nm and 865 nm. The tendency is confirmed by comparisons to the MERIS TOA reflectance (only 7 doublets) indicating degradations of 7% per year at 443 nm, 6 % per year at 490 nm, 3 % per year at 560 nm, 4 % per year at 670 nm and 2 % per year 865 nm. These figures are not conclusive and need to be confirmed by longer time series.

5 CONCLUSION

The results of the here presented simple methodology seem to show that MERIS and A-MODIS are radiometrically in line. In comparison to these sensors, the SeaWiFS data lie 10 % lower. AATSR compares relatively well to MERIS and A-MODIS but shows, as expected from the still-to-be-performed update of the degradation model, a decrease of sensitivity in 2005 at 560 nm and 607 nm. The results of these intercomparisons also seem to indicate a degradation of the POLDER-3 sensitivity of several percents through its first year of operation that need to be confirmed by longer time series.

6 ACKNOWLEDGMENT

Thanks to Olga Faber (Brockmann Consult) for providing and screening MERIS data. Thanks to Alessandra Tassa for proposing to clean up messy items at Uyuni. MODIS and SeaWiFS data were obtained from the NASA Langley Research Center Atmospheric Sciences Data Center. AATSR and MERIS data were provided by the European Space Agency. The POLDER-3 data were provided by the Centre National d'Etudes Spatiales.

7 REFERENCES

R 1 Barnes Robert A., Robert E. Eplee, Jr., Frederick S. Patt, and Charles R. McClain, Changes in the radiometric sensitivity of SeaWiFS determined from lunar and solar-based measurements, 20 July 1999, Vol. 38, No. 21, *Applied Optics*, p. 4649

R 2 Barnes Robert A., Robert E. Eplee, Jr., G. Michael Schmidt, Frederick S. Patt, and Charles R. McClain, Calibration of SeaWiFS. I. Direct techniques, *Applied Optics. 40, 6682-6700, 2001*

R 3 Berk, A. G. P. Anderson, P. K. Acharya, J. H. Chetwynd, L. S. Bernstein, E. P. Shettle, M. W. Matthew, and S. M. Adler-Golden, MODTRAN4 User's Manual, Abreu L. W. and Anderson G. P. (Eds.), Air Force Research Laboratory, Space Vehicles Directorate, Hanscom AFB, MA, pp: 97, 1999 (revised April 2000).

R 4 Bouvet M., S. Delwart, Imaging spectrometers comparison over snow – A case study over Longyearbyen on the 3rd of May 2003, *Envisat MAVT 2003 proceedings*

R 5 Chandrasekhar S., Radiative transfer, *Dover publications*, Inc, 1960.

R 6 Cosnefroy, H, Soule, P., Briottet, X., Hagolle, O., Cabot, F. POLDER multiangular calibration using desert sites: method and performances, Proceedings of SPIE Volume: 3221, 1997

R 7 Delwart S., Preusker, Ludovic Bourg, Richard Santer, Didier Ramon, Jurgen Fischer (2006), MERIS in-flight spectral calibration, *International Journal of Remote Sensing, MERIS special issue* (accepted in 2005).

R 8 Eplee et al. (2001), "Calibration of SeaWiFS. II. Vicarious techniques," *Applied Optics*, Vol. 40, 6701-6718.

R 9 Goryl Philippe and Saunier Sebastien, Analysis of the absolute location accuracy of MERIS FR (Full Resolution) level 1B products, 2004, (http://earth.esa.int/pcs/envisat/meris/documentation/GAEL-P179-TCN-006-01-00-Meris_Absolute_location_control_report.pdf)

R 10 Gregg, W. and Carder K. L., A simple spectral solar irradiance model for cloudless maritime atmospheres, *Limnology and oceanography*, vol. 35, no. 8, dec 1990.

R 11 Hagolle O., P. Goloub, P.-Y. Deschamps, H. Cosnefroy, X. Briottet, T. Bailleul, J.M.Nicolas, F. Parol, B. Lafrance, and M. Herman, "Results of POLDER In-Flight Calibration," *IEEE Transactions on Geoscience and Remote Sensing*, vol. 37, pp. 1550-1566, 1999.

R 12 Hagolle O., Cabot F., Absolute calibration of MERIS using natural targets, *Proceeding of the MERIS AATSR Validation Team Meeting 2003*.

R 13 Hooker, S.B., W.E. Esaias, G.C. Feldman, W.W. Gregg, and C.R. McClain, 1992: An Overview of SeaWiFS and Ocean Color. *NASA Tech. Memo. 104566, Vol. 1*, S.B. Hooker and E.R. Firestone, Eds., NASA Goddard Space Flight Center, Greenbelt, Maryland, 24 pp., plus color plates.

R 14 Isaacman A., G. Toller, B. Guenther, W.L. Barnes and X. Xiong, MODIS Level 1B calibration and data products, *Proceedings of SPIE ˆ Earth Observing Systems VIII*, 5151, 552-562, 2003

R 15 Lamparelli Rubens Augusto Camargo, Flávio Jorge Ponzoni, Jurandir Zullo, Jr., Giampaolo Queiroz Pellegrino, and Yves Arnaud, Characterization of the Salar de Uyuni for In-Orbit Satellite Calibration, *IEEE TRANSACTIONS ON GEOSCIENCE AND REMOTE SENSING*, VOL. 41, NO. 6, June 2003

R 16 Martiny N, R. Frouin, and R. Santer, Radiometric calibration of SeaWiFS in the near infrared, Applied Optics 44, 7828-7844 (2005)

R 17 MERIS and AATSR Product handbook can be found at www.envisat.esa.int

R 18 Nieke J., M. Hori, R. Holler, I. Asanuma, Satellite sensor inter-calibration - A case study for 28 March 2002, *ENVISAT Validation Workshop Proceedings December 2002*

R 19 PARASOL/POLDER site: http://parasol-polder.cnes.fr/en/index.htm

R 20 PCF MERIS Team and QWG, MERIS SMILE effect characterization and correction, ESA document, May 2005 (see http://earth.esa.int/pcs/envisat/meris/documentation/MERIS_Smile_Effect.pdf)

R 21 Rast M., Bezy J.L., and Bruzzi S., 1999: The ESA Medium Resolution Imaging Spectrometer MERIS: a review of the instrument and its mission. *International Journal of Remote Sensing.*, 20, 1681-1702 pp.

R 22 Smith D., Optical sensors inter-comparison, *proceedings of the MERIS AATSR Valitation Team Workshop 2006*

R 23 Thuillier, G., M. Hersé, P. C. Simon, D. Labs, H. Mandel, D. Gillotay, and T. Foujols, 2003, "The solar spectral irradiance from 200 to 2400 nm as measured by the SOLSPEC spectrometer from the ATLAS 1-2-3 and EURECA missions, *Solar Physics*, 214(1): 1-22.

R 24 Tinel C., Vicarious Calibration over Deserts sites, *proceedings of the MERIS AATSR Valitation Team Workshop 2006*

R 25 Xiong X., K. Chiang, J. Esposito, B. Guenther and W.L. Barnes, MODIS On-orbit Calibration and Characterization, *Metrologia* 40, 89-92, 2003

R 26 Xiong X, J.Sun, J.Esposito, B.Guenther and W.Barnes, MODIS Reflective Solar Bands Calibration Algorithm and On-orbit Performance. *Proceeding of SPIE China* (2004)